Observer-based MPC Design of an Axial Dispersion Tubular Reactor: Addressing Recycle Delays through Transport PDEs

Behrad Moadeli and Stevan Dubljevic[1]

***Abstract*— The model predictive control of an axial dispersion tubular reactor equipped with a recycle stream is presented. The intrinsic time delay imposed by the recycle stream, an often overlooked aspect in chemical engineering process control studies, is modeled as a transport PDE, leading to a boundary-controlled system of coupled parabolic and hyperbolic PDEs under Danckwerts boundary conditions, suitable for this reactor type. Considering the digital nature of modern controllers, a discrete-time linear model predictive controller is designed to stabilize the system, coupled with a Luenberger state estimator to address the controller's limited access to the system's full state. The need for model reduction through spatial approximation is eliminated by following a late lumping approach, while utilizing Cayley-Tustin time discretization method to preserve the continuous-time system's characteristics. The controller's effectiveness is demonstrated through numerical simulations, showcasing its capability to stabilize an unstable system while adhering to input constraints, having access merely to output measurements.**

I. Introduction

Many chemical and petrochemical processes involve states that evolve over both space and time. These processes are modeled as distributed parameter systems (DPSs) using partial differential equations (PDEs) [1]. The infinite-dimensional nature of DPSs poses distinct challenges for control and estimation. Two primary strategies exist for addressing this: Early Lumping and Late Lumping. Early Lumping discretizes the system early in the modeling process to enable standard control techniques [2], but this can introduce inaccuracies due to model reduction errors [3]. In contrast, Late Lumping retains the system's infinite-dimensional structure until the final controller implementation stage, offering higher fidelity at the cost of greater complexity.

Several Late Lumping approaches have been employed to control convection-reaction and diffusion-convection-reaction systems modeled by hyperbolic and parabolic PDEs, respectively. Robust and boundary feedback control of plug flow reactors have been demonstrated in [4], [5], while [6] addresses state feedback design for countercurrent heat exchangers. The role of dispersion in axial dispersion tubular reactors is considered in [7], and low-dimensional predictive controllers based on modal decomposition have been explored in [8]. A comprehensive observer-based MPC strategy is proposed in [9] for axial dispersion tubular reactors with recycle, combining diffusion, convection, and feedback under input constraints. State reconstruction for DPSs has also been addressed using discrete-time Luenberger observers without spatial discretization, a key feature consistent with the late lumping paradigm [10]–[13].

Delay systems, another class of infinite-dimensional systems, are often represented either as delay differential equations or transport PDEs, with the latter offering advantages in systems with spatial dynamics [14]. While input/output delays have been widely studied in chemical engineering using cascade PDE models [15]–[17], state delays are less commonly addressed. Notable exceptions include heat exchanger systems with stream passage delays [18] and plug flow reactors with recycle delays that omit dispersion [19]. Regarding diffusion-convection-reaction systems, even the work of [9]—which remains one of the most complete applications of Late Lumping for distributed chemical reactors—assumes an instantaneous recycle stream, leaving a gap in the literature concerning systems where recycle imposes a state delay.

This work addresses an axial dispersion tubular reactor with recycle, modeled as a coupled system of parabolic and hyperbolic PDEs to capture both spatial dispersion and recycle-induced state delay. A closed-form resolvent operator is derived to preserve the system's infinite-dimensional structure using the Late Lumping approach. The system is then discretized using the Cayley-Tustin method, a Crank-Nicolson-type scheme that conserves the dynamics without requiring model reduction [20], [21]. A discrete-time infinite-dimensional Luenberger observer is designed to reconstruct unmeasured states, enabling output feedback MPC. Simulations show that the proposed controller successfully stabilizes the otherwise unstable system under input constraints.

II. Continuous-time Model Representation

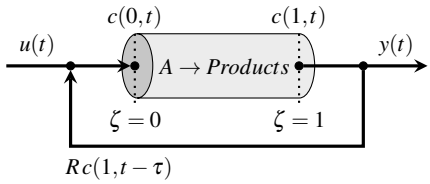

Fig. 1. Axial tubular reactor with recycle stream.

Figure 1 illustrates the chemical process within an axial dispersion tubular reactor equipped with a recycle stream,

[1]Behrad Moadeli and Stevan Dubljevic are with the Department of Chemical and Materials Engineering, University of Alberta, Edmonton, AB, Canada T6G 1H9 moadeli@ualberta.ca, stevan.dubljevic@ualberta.ca

Funding provided by the Natural Sciences and Engineering Research Council of Canada—NSERC (RGPIN-2022-03486).

where a general nonlinear reaction occurs [22]. A fraction of the outlet stream is recycled and mixed with the fresh input to enhance substrate conversion. By applying mass balance over an infinitesimal element along the reactor axis and linearizing the reaction term around a steady state, the system dynamics can be expressed as a second-order parabolic PDE with a delayed boundary condition. Dankwerts-type boundary conditions are used to account for non-ideal mixing and flow behavior [23], while the recycle stream introduces a state delay at the reactor inlet. The full modeling rationale—including boundary condition selection, linearization procedure, and physical assumptions—follows our prior work [24], to which the reader is referred for further detail. The resulting PDE system is as follows:

$$\begin{aligned} &\dot{c}(\zeta,t) = D\,\partial_\zeta^2 c(\zeta,t) - v\,\partial_\zeta c(\zeta,t) - k_r\,c(\zeta,t) \\ &\begin{cases} D\,\partial_\zeta c(0,t) - v\,c(0,t) = -v\left[R c(1,t-\tau) + (1-R)\,u(t)\right] \\ \partial_\zeta c(1,t) = 0 \\ y(t) = c(1,t) \end{cases} \end{aligned} \tag{1}$$

Here, $c(\zeta,t)$ denotes the deviation of concentration from the steady state along the reactor length. The parameters D, v, k_r, R, and τ represent the diffusion coefficient, flow velocity, linearized reaction coefficient, recycle ratio, and residence time of the recycle stream, respectively. The spatial and temporal domains are $\zeta \in [0,1]$ and $t \in [0,\infty)$.

An interesting approach to address delays where the problem involves other forms of PDEs is to reformulate the problem such that the notion of delay is replaced with an alternative transport PDE [14]. Therefore, the state variable $c(\zeta,t)$ is replaced with a new state variable $\underline{x}(\zeta,t) \equiv [x_1(\zeta,t), x_2(\zeta,t)]^T$ as a vector of functions, where $x_1(\zeta,t)$ represents the concentration within the reactor—analogous to $c(\zeta,t)$—and $x_2(\zeta,t)$ is the new state variable for the concentration along the recycle stream. The system output will consequently be defined as $y(t) = x_1(1,t)$. In addition, the delay can be modeled as a pure transport process rather than being present in the argument of the state at the boundary—i.e. $c(1,t-\tau)$— making all state variables expressed explicitly at a specific time instance t, resulting in the standard state-space form for an infinite-dimensional linear time-invariant (LTI) system given in (2).

$$\begin{aligned} \dot{\underline{x}}(\zeta,t) &= \mathfrak{A}\underline{x}(\zeta,t) + \mathfrak{B}u(t) \\ y(t) &= \mathfrak{C}\underline{x}(\zeta,t) + \mathfrak{D}u(t) \end{aligned} \tag{2}$$

Here, $\mathfrak{A}$ is a linear operator $\mathscr{L}(X)$ acting on a Hilbert space $X : L^2[0,1] \times L^2[0,1]$ and $\underline{x}(\zeta,t)$, as defined previously, is the vector of functions describing the states of the system. Input operator $\mathfrak{B}$ is a linear operator that maps the scalar input from input-space onto the state space. Output operator $\mathfrak{C}$ on the other hand, is a linear operator that maps the infinite-dimensional state space onto the finite-dimensional output space, resulting in a scalar output. The operator $\mathfrak{D}$ is the direct transmission operator, which is set to zero in this case as there is no direct transmission from the input to the output in the continuous-time system. The operators ($\mathfrak{A}$, $\mathfrak{B}$, $\mathfrak{C}$, and $\mathfrak{D}$) are shown in (3) for the infinite-dimensional LTI system.

$$\begin{aligned} \mathfrak{A} &\equiv \begin{bmatrix} D\partial_{\zeta\zeta} - v\partial_\zeta + k_r & 0 \\ 0 & \frac{1}{\tau}\partial_\zeta \end{bmatrix} \\ D(\mathfrak{A}) &= \Big\{ \underline{x}(\zeta) = [x_1(\zeta), x_2(\zeta)]^T \in X : \\ &\quad \underline{x}(\zeta), \partial_\zeta \underline{x}(\zeta), \partial_{\zeta\zeta}\underline{x}(\zeta) \quad \text{a.c.}, \\ &\quad D\partial_\zeta x_1(0) - v x_1(0) = -vRx_2(0), \\ &\quad \partial_\zeta x_1(1) = 0, x_1(1) = x_2(1) \Big\} \\ \mathfrak{B} &\equiv \begin{bmatrix} \delta(\zeta) \\ 0 \end{bmatrix} v(1-R) \\ \mathfrak{C} &\equiv \begin{bmatrix} \int_0^1 \delta(\zeta-1)(\cdot)d\zeta & 0 \end{bmatrix} \\ \mathfrak{D} &= 0 \end{aligned} \tag{3}$$

with $\delta(\zeta)$ being dirac delta function. The system's spectrum can now be obtained by solving the eigenvalue problem for the system generator $\mathfrak{A}$. To do this, the characteristics equation of the system needs to be obtained by solving the equation $det(\mathfrak{A} - \lambda_i\ I) = 0$ for λ_i, where $\lambda_i \in \mathbb{C}$ is the i^{th} eigenvalue of the system and I is the identity operator. Attempts to analytically solve this equation will fail; therefore, it is solved numerically given the parameters in Table I. The eigenvalue distribution is given in Figure 2 in the complex plane. This suggests that the open-loop system is unstable, as there are eigenvalues with positive real parts.

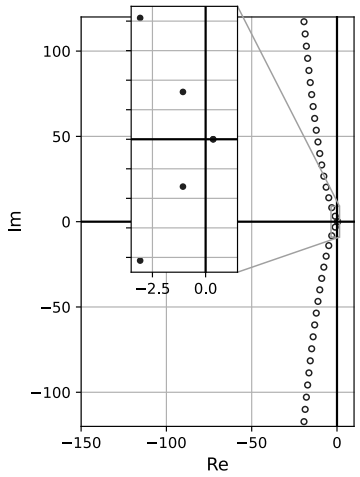

Fig. 2. Eigenvalues of operator $\mathfrak{A}$.

TABLE I
PHYSICAL PARAMETERS FOR THE SYSTEM

Parameter	Symbol	Value	Unit
Diffusivity	D	2×10^{-5}	m^2/s
Velocity	v	0.01	m/s
Reaction Constant	k_r	-1.5	s^{-1}
Recycle Residence Time	τ	80	s
Recycle Ratio	R	0.3	$-$

The exact closed-form representation for the resolvent operator is derived in Appendix A. Since the system is not

self-adjoint, the adjoint system operators $\mathfrak{A}^*$ and $\mathfrak{B}^*$ as well as the resolvent operator for the adjoint system must be obtained in the same manner as the original system. However, this is not included in the manuscript to avoid redundancy.

III. Cayley-Tustin Time Discretization

Having access to the resolvent operators of the original and the adjoint system, the Cayley-Tustin time-discretization can be utilized to map the continuous-time setting to the discrete-time setting without losing crucial dynamical properties of the system, such as stability and controllability. This Crank-Nicolson type of discretization is also known as the lowest order symplectic integrator in Gauss quadrature-based Runge-Kutta methods [25]. Considering Δt as the sampling time, and assuming a piecewise constant input within time intervals (a.k.a. zero-order hold), the discrete-time representation $\underline{x}(\zeta,k) = \mathfrak{A}_d\underline{x}(\zeta,k-1) + \mathfrak{B}_d u(k)$ is obtained, with discrete-time operators $\mathfrak{A}_d$ and $\mathfrak{B}_d$ defined in (4), where $\alpha = 2/\Delta t$. As required for systems with nonself-adjoint generators, the adjoint discrete-time operators $\mathfrak{A}_d^*$ and $\mathfrak{B}_d^*$ are also obtained in a similar manner.

$$\begin{bmatrix}\mathfrak{A}_d & \mathfrak{B}_d\\ \mathfrak{C}_d & \mathfrak{D}_d\end{bmatrix} = \begin{bmatrix}-I+2\alpha\mathfrak{R}(\alpha,\mathfrak{A}) & \sqrt{2\alpha}\mathfrak{R}(\alpha,\mathfrak{A})\mathfrak{B}\\ \sqrt{2\alpha}\mathfrak{C}\mathfrak{R}(\alpha,\mathfrak{A}) & \mathfrak{C}\mathfrak{R}(\alpha,\mathfrak{A})\mathfrak{B}\end{bmatrix} \tag{4}$$

IV. Observer Design

One important issue of DPSs is the limited access to the states of the infinite-dimensional system as the state is distributed over the entire domain and performing infinite measurements is never feasible. Therefore, an observer is required to estimate the states of the system based on the available measurements. To address this issue, a Luenberger observer is designed to reconstruct the states of the system based on the output measurements. First, the continuous-time observer design is considered; followed by the design of the discrete-time observer.

A. Continuous-Time Observer Design

For the purpose of state reconstruction of a diffusion-convection-reaction system, where the feedforward term $\mathfrak{D}$ is generally absent, the continuous-time observer dynamics are given by (5).

$$\begin{aligned}\dot{\underline{\hat{x}}}(\zeta,t) &= \mathfrak{A}\underline{\hat{x}}(\zeta,t) + \mathfrak{B}u(t) + \mathfrak{L}_c[y(t)-\hat{y}(t)]\\ \hat{y}(t) &= \mathfrak{C}\underline{\hat{x}}(\zeta,t)\end{aligned} \tag{5}$$

where $\hat{\underline{x}}(\zeta,t)$ is the reconstructed state of the original system and $\mathfrak{L}_c$ is the continuous-time observer gain. By subtracting the observer dynamics from the original system dynamics, the error dynamics $e(\zeta,t)$ are obtained as shown in (6).

$$\dot{e}(\zeta,t) = (\mathfrak{A}-\mathfrak{L}_c\mathfrak{C})e(\zeta,t) \equiv \mathfrak{A}_o e(\zeta,t) \tag{6}$$

The goal is to design the observer gain $\mathfrak{L}_c$ such that the error dynamics are exponentially stable, i.e. $\max\{\mathrm{Re}(\lambda_o)\} < 0$ where $\{\lambda_o\}$ is the set of eigenvalues of the error dynamics operator $\mathfrak{A}_o$. Three different forms of the observer gain are considered as spatial functions $\mathfrak{L}_c = f(\zeta, l_{obs})$ with the effect of the scalar coefficient l_{obs} on $\max\{\mathrm{Re}(\lambda_o)\}$ shown in Fig. 3.

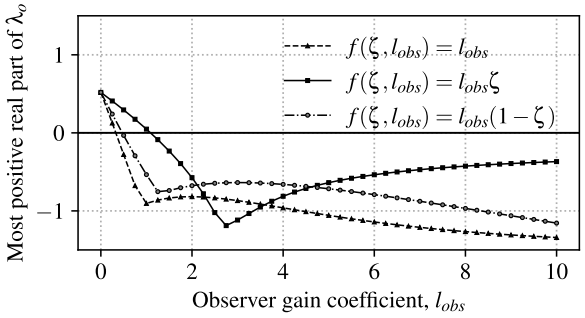

Fig. 3. The effect of various observer gains $\mathfrak{L}_c = f(\zeta, l_{obs})$ on the eigenvalues of state reconstruction error dynamics λ_o.

B. Discrete-Time Observer Design

Once an appropriate continuous-time observer gain is determined, the discrete-time observer gain $\mathfrak{L}_d$ may be obtained using the same Cayley-Tustin time discretization approach, as shown in (7).

$$\begin{aligned}\underline{\hat{x}}(\zeta,k) &= \mathfrak{A}_d\underline{\hat{x}}(\zeta,k-1) + \mathfrak{B}_d u(k) + \mathfrak{L}_d[y(k)-\hat{y}(k)]\\ \hat{y}(k) &= \mathfrak{C}_{d,o}\underline{\hat{x}}(\zeta,k-1) + \mathfrak{D}_{d,o}u(k) + \mathfrak{M}_{d,o}y(k)\end{aligned} \tag{7}$$

with $\mathfrak{A}_d$ and $\mathfrak{B}_d$ defined in (4), and $\mathfrak{C}_{d,o}$, $\mathfrak{D}_{d,o}$, $\mathfrak{M}_{d,o}$, and $\mathfrak{L}_d$ are given in (8).

$$\begin{aligned}\mathfrak{C}_{d,o}(\cdot) &= \sqrt{2\alpha}\left[I+\mathfrak{C}(\alpha I-\mathfrak{A})\mathfrak{L}_c\right]^{-1}\mathfrak{C}\mathfrak{R}(\alpha,\mathfrak{A})(\cdot)\\ \mathfrak{D}_{d,o} &= \left[I+\mathfrak{C}(\alpha I-\mathfrak{A})\mathfrak{L}_c\right]^{-1}\mathfrak{C}\mathfrak{R}(\alpha,\mathfrak{A})\mathfrak{B}\\ \mathfrak{M}_{d,o} &= \left[I+\mathfrak{C}(\alpha I-\mathfrak{A})\mathfrak{L}_c\right]^{-1}\mathfrak{C}\mathfrak{R}(\alpha,\mathfrak{A})\mathfrak{L}_c\\ \mathfrak{L}_d &= \sqrt{2\alpha}\mathfrak{R}(\alpha,\mathfrak{A})\mathfrak{L}_c\end{aligned} \tag{8}$$

It can been shown that using this approach, the discrete-time error dynamics will be stable if the continuous-time observer gain $\mathfrak{L}_c$ is chosen such that $\mathfrak{A}_o$ is stable. It is also worth noting that the proposed methodology skips the need for model reduction associated with the discrete-time Luenberger observer, with no spatial approximation required as well [9]–[13].

V. Model Predictive Controller Design

In this section, the observer-based MPC shown in Fig. 4 is developed with the goal of stabilizing the given unstable infinite-dimensional system within an optimal framework, relying solely on output measurements while satisfying input constraints. An infinite-time open-loop objective function sets the foundation of the controller design in the discrete-time setting at each sampling instant k. The objective function consists of a weighted sum of actuation costs as well as state deviations, for all future time instances, subject to the system dynamics and input constraints. Since full-state is assumed to be unavailable, reconstructed states are used to estimate states of the system, as shown in (9).

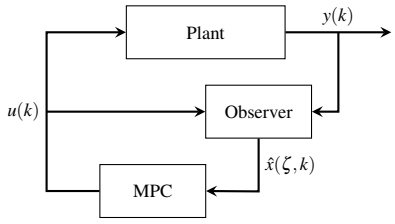

Fig. 4. Block diagram representation of the observer-based MPC.

$$\begin{aligned}\min_{U} \quad & \sum_{l=0}^{\infty} \langle \underline{\hat{x}}(\zeta,k+l|k), \mathfrak{Q}\underline{\hat{x}}(\zeta,k+l|k)\rangle \\ & +\langle u(k+l+1|k), \mathfrak{F}u(k+l+1|k)\rangle \\ \text{s.t.} \quad & \underline{\hat{x}}(\zeta,k+l|k) = \mathfrak{A}_d\underline{\hat{x}}(\zeta,k+l-1|k) + \mathfrak{B}_d u(k+l|k) \\ & u^{min} \le u(k+l|k) \le u^{max}\end{aligned} \tag{9}$$

where $\mathfrak{Q}$ and $\mathfrak{F}$ are positive definite operators of appropriate dimensions, responsible for penalizing state deviations and actuation costs, respectively. The notation $(k+l|k)$ indicates the future time states or input instance $k+l$ obtained at time k. The infinite-time optimization problem may be reduced to a finite-time setup by assigning zero-input beyond a certain control horizon N, resulting in the optimization problem in (10).

$$\begin{aligned}\min_{U} \quad & \sum_{l=0}^{N-1} \langle \underline{\hat{x}}(\zeta,k+l|k), \mathfrak{Q}\underline{\hat{x}}(\zeta,k+l|k)\rangle \\ & +\langle u(k+l+1|k), \mathfrak{F}u(k+l+1|k)\rangle \\ & +\langle \underline{\hat{x}}(\zeta,k+N|k), \mathfrak{P}\underline{\hat{x}}(\zeta,k+N|k)\rangle \\ \text{s.t.} \quad & \underline{\hat{x}}(\zeta,k+l|k) = \mathfrak{A}_d\underline{\hat{x}}(\zeta,k+l-1|k) + \mathfrak{B}_d u(k+l|k) \\ & u^{min} \le u(k+l|k) \le u^{max} \\ & \langle \underline{\hat{x}}(\zeta,k+N|k), \underline{\phi_u}(\zeta)\rangle = 0\end{aligned} \tag{10}$$

where $\mathfrak{P}$ is the terminal cost operator obtained as the solution to the discrete-time Lyapunov equation, as shown in (11). This operator can be shown to be positive definite only if the terminal state $\underline{\hat{x}}(\zeta,k+N|k)$ is in a stable subspace. Therefore, for the resulting quadratic optimization problem to be convex, an equality constraint is introduced to guarantee $\mathfrak{P}$ is positive definite. The terminal constraint is enforced by setting the projection of the terminal state onto the unstable subspace of the system to zero [9], [21], [26].

$$\mathfrak{P}(\cdot) = \sum_{m=0}^{\infty}\sum_{n=0}^{\infty} -\frac{\langle \underline{\phi_m}, \mathfrak{Q}\underline{\psi_n}\rangle}{\lambda_m + \overline{\lambda_n}} \langle (\cdot), \underline{\psi_n}\rangle \phi_m \tag{11}$$

Here, $\underline{\phi_u}(\zeta)$ denotes the set of unstable eigenfunctions of the system, corresponding to all eigenvalues with $\mathrm{Re}(\lambda_u) \ge 0$. In addition, $\underline{\phi_i}$ and $\underline{\psi_i}$ represent the i^{th} eigenfunctions of the original and adjoint systems, respectively. The resulting finite-horizon control problem can be algebraically manipulated into a format compatible with conventional quadratic programming (QP) solvers, where the input sequence over the prediction horizon N is defined as

$$U = \begin{bmatrix} u(k+1|k) & u(k+2|k) & \dots & u(k+N|k)\end{bmatrix}^{\top}.$$

At each sampling instant k, the optimal input sequence U is obtained by solving the QP. However, only the first control input, $u(k+1|k)$, is applied to the system in accordance with the receding horizon strategy. Upon receiving the next output measurement $y(k+1)$, the Luenberger observer reconstructs the current system state at time $k+1$, which then initializes the next optimization cycle. This loop repeats at every time step, enabling real-time output feedback control while reconstructing system states. See Appendix B for mathematical details of the QP formulation.

VI. Results and Discussion

Numerical simulations for the closed-loop system under the proposed observer-based output feedback MPC are presented in this section, with parameters chosen according to Table I. As the eigenvalue distribution obtained in Fig(2) suggests, the open-loop system is unstable due to the presence of an eigenvalue with positive real part.

An infinite-dimensional MPC is designed and applied to the system with the initial condition for the reactor set to $c(\zeta,0) = \sin^2(\pi\zeta)$. The recycle stream is assumed to be empty at the beginning of the simulation. The state deviation and actuation penalty terms are set as $\mathfrak{Q} = 0.04I$ and $\mathfrak{F} = 27$. The sampling time and the horizon length for the MPC are set to $\Delta t = 20$ s and $N = 9$, respectively, while the input constraints are assumed to be $0 \le u(t) \le 0.15$. The initial condition for estimated states are assumed to be zero all over the domain. Lastly, the observer gain is set to a constant function $\mathfrak{L}_c = 1$.

The closed-loop response of the system is shown in Fig(5) and the control input as well as the system output is shown in Fig(6). State reconstruction error dynamics of the proposed Luenberger observer is also shown in Fig(7). According to the results, it can be confirmed that the observer-based MPC successfully stabilizes the unstable system using solely output measurements while satisfying the input constraints.

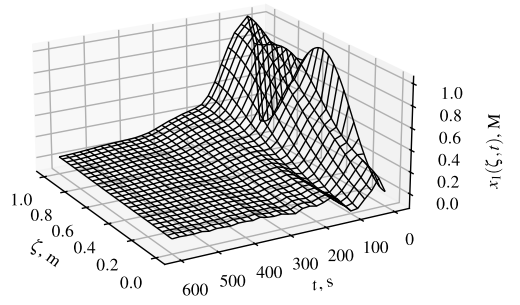

Fig. 5. Stabilized reactor concentration profile under the proposed MPC.

One important aspect of the proposed observer-based controller is to confirm how the state reconstruction error dynamics stabilize faster compared to the closed-loop system dynamics. This will avoid unwanted oscillations that will

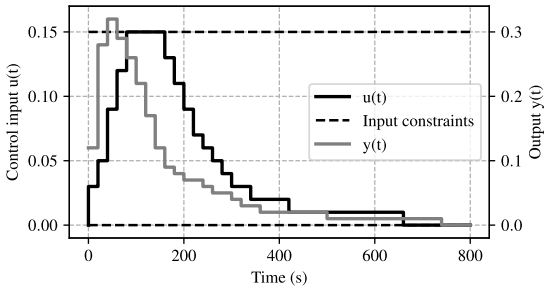

Fig. 6. Input constraints, the obtained input profile, and the reactor output under the proposed MPC.

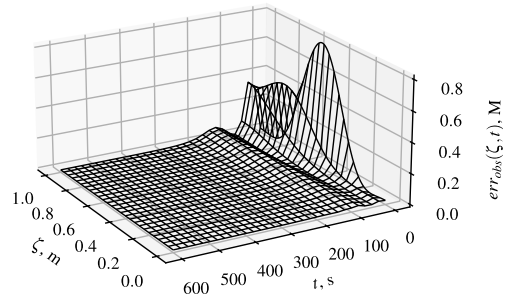

Fig. 7. State reconstruction error profile of the proposed Luenberger observer along the reactor.

affect the performance of the controller due to poor state estimations. In addition, oscillations may arise in the system dynamics due to the presence of the recycle stream. While the axial dispersion reactors show no oscillation in the absence of recycle, the nature of recycle streams introduces such behavior in either the open-loop system or a closed-loop system where the control horizon is short relative to the state-delay imposed by the recycle stream. In this example, the control horizon, i.e. 180 s, is set to be considerably longer than the recycle delay, which is 80 s; resulting in a non-oscillatory input profile as the model-based controller is able to capture the effect of the recycle stream on the system dynamics.

APPENDIX

A. Resolvent Operator Derivation

To obtain the closed form of the resolvent operator $\mathfrak{R}(s,\mathfrak{A}) = (sI-\mathfrak{A})^{-1}$, it can be treated as an operator that maps the initial condition or the input to the Laplace transform of the state of the system $\underline{X}(\zeta,s)$. In (12), Laplace transform is applied to the LTI representation of the system for both zero-input response and zero-state response to obtain a general expression for the resolvent operator. The goal is to obtain the solution for $\underline{X}(\zeta,s)$ and compare it with the general expression obtained in (12) to get the closed form expression for the resolvent operator. First step is to apply Laplace transform to the original system of PDEs in (3).

$$\begin{aligned}
&\dot{\underline{x}}(\zeta,t) = \mathfrak{A}\underline{x}(\zeta,t) + \mathfrak{B}u(t) \xrightarrow{\mathscr{L}} \\
&s\underline{X}(\zeta,s) - \underline{x}(\zeta,0) = \mathfrak{A}\underline{X}(\zeta,s) + \mathfrak{B}U(s) \\
&\begin{cases} \xrightarrow{u=0} & \underline{X}(\zeta,s) = (sI-\mathfrak{A})^{-1}\underline{x}(\zeta,0) = \mathfrak{R}(s,\mathfrak{A})\underline{x}(\zeta,0) \\ \xrightarrow{\underline{x}(0,\zeta)} & \underline{X}(\zeta,s) = (sI-\mathfrak{A})^{-1}\mathfrak{B}U(s) = \mathfrak{R}(s,\mathfrak{A})\mathfrak{B}U(s) \end{cases}
\end{aligned} \tag{12}$$

The second order derivative term is decomposed to two first order PDEs, constructing a new 3×3 system of first order ODEs with respect to ζ after Laplace transformation, as shown in (13) along with the solution.

$$\begin{aligned}
&\partial_\zeta \overbrace{\begin{bmatrix} X_1(\zeta,s) \\ \partial_\zeta X_1(\zeta,s) \\ X_2(\zeta,s) \end{bmatrix}}^{\tilde{\underline{X}}(\zeta,s)} = \overbrace{\begin{bmatrix} 0 & 1 & 0 \\ \frac{s-k}{D} & \frac{v}{D} & 0 \\ 0 & 0 & s\tau \end{bmatrix}}^{P(s)} \begin{bmatrix} X_1(\zeta,s) \\ \partial_\zeta X_1(\zeta,s) \\ X_2(\zeta,s) \end{bmatrix} \\
&\qquad + \underbrace{\begin{bmatrix} 0 \\ -\frac{x_1(\zeta,0)}{D} + v(1-R)\delta(\zeta)U(s) \\ -\tau x_2(\zeta,0) \end{bmatrix}}_{Z(\zeta,s)} \\
&\Rightarrow \tilde{\underline{X}}(\zeta,s) = \underbrace{e^{P(s)\zeta}}_{T(\zeta,s)}\tilde{\underline{X}}(0,s) + \int_0^\zeta \underbrace{e^{P(s)(\zeta-\eta)}}_{F(\zeta,\eta)} Z(\eta,s)d\eta
\end{aligned} \tag{13}$$

Since the boundary conditions are not homogeneous, $\tilde{\underline{X}}(0,s)$ needs to be obtained by solving the system of algebraic equations given in (14).

$$\begin{aligned}
&\overbrace{\begin{bmatrix} -v & D & Rv \\ T_{11}(1,s) & T_{12}(1,s) & -T_{33}(1,s) \\ T_{21}(1,s) & T_{22}(1,s) & 0 \end{bmatrix}}^{M^{-1}(s)} \tilde{\underline{X}}(0,s) = \\
&\underbrace{\int_0^1 \begin{bmatrix} 0 \\ F_{33}(1,\eta)Z_3(\eta,s) - F_{12}(1,\eta)Z_2(\eta,s) \\ -F_{22}(1,\eta)Z_2(\eta,s) \end{bmatrix} d\eta}_{\underline{b}(s)}
\end{aligned} \tag{14}$$

Having access to $\tilde{\underline{X}}(0,s)$, the resolvent operator can be explicitly derived as shown in (15) and (16) for zero-state and zero-input cases, respectively.

$$\begin{aligned}
&\underline{x}(\zeta,0) = 0 \Rightarrow \mathfrak{R}(s,\mathfrak{A})\mathfrak{B}(\cdot) = \begin{bmatrix} \mathfrak{R}_1\mathfrak{B} \\ \mathfrak{R}_2\mathfrak{B} \end{bmatrix}(\cdot) \Rightarrow \\
&\mathfrak{R}_1\mathfrak{B} = -v(1-R)\Big[\sum_{j=1}^{2} T_{1j}(\zeta)(M_{j2}T_{12}(1) + M_{j3}T_{22}(1)) \\
&\qquad - T_{12}(\zeta)\Big](\cdot) \\
&\mathfrak{R}_2\mathfrak{B} = -v(1-R)\left[T_{33}(\zeta)(M_{32}T_{12}(1) + M_{33}T_{22}(1))\right](\cdot)
\end{aligned} \tag{15}$$

$$
\begin{aligned}
&U(s)=0 \Rightarrow \mathfrak{R}(s,\mathfrak{A})\underline{(\cdot)}=\begin{bmatrix}\mathfrak{R}_{11} & \mathfrak{R}_{12}\\ \mathfrak{R}_{21} & \mathfrak{R}_{22}\end{bmatrix}\begin{bmatrix}(\cdot)_1\\(\cdot)_2\end{bmatrix}\Rightarrow\\
&\mathfrak{R}_{11}=\sum_{j=1}^{2}\frac{T_{1j}(\zeta)}{D}\int_0^1\left[M_{j2}F_{12}(1,\eta)+M_{j3}F_{22}(1,\eta)\right](\cdot)_1 d\eta\\
&\qquad-\frac{1}{D}\int_0^{\zeta}F_{12}(\zeta,\eta)(\cdot)_1 d\eta\\
&\mathfrak{R}_{12}=\sum_{j=1}^{2}-\tau T_{1j}(\zeta)\int_0^1 M_{j2}F_{33}(1,\eta)(\cdot)_2 d\eta\\
&\mathfrak{R}_{21}=\frac{T_{33}(\zeta)}{D}\int_0^1\left[M_{32}F_{12}(1,\eta)+M_{33}F_{22}(1,\eta)\right](\cdot)_1 d\eta\\
&\mathfrak{R}_{22}=-\tau T_{33}(\zeta)\int_0^1 M_{32}F_{33}(1,\eta)(\cdot)_2 d\eta\\
&\qquad-\tau\int_0^{\zeta}F_{33}(\zeta,\eta)(\cdot)_2 d\eta
\end{aligned}
\tag{16}
$$

B. Standard QP Representation for the MPC Optimization Problem

Simple algebraic manipulation can be performed to express future state trajectories in terms of the current estimated state and a sequence of future inputs, allowing the optimization problem in (10) to be reformulated into the standard quadratic programming (QP) structure shown in (17). This reformulation enables the use of conventional QP solvers for efficient real-time implementation.

$$
\begin{aligned}
&\min_{U} J = U^{\top}\langle I,H\rangle U + 2U^{\top}\langle I,P\underline{\hat{x}}(\zeta,k|k)\rangle\\
&\text{s.t.}\qquad U^{min}\le U\le U^{max}\\
&\qquad\quad T_u\underline{\hat{x}}(\zeta,k|k)+S_uU=0\\
&\text{with } H=\\
&\begin{bmatrix}
\mathfrak{B}_d^*\mathfrak{P}\mathfrak{B}_d+\mathfrak{F} & \mathfrak{B}_d^*\mathfrak{A}_d^*\mathfrak{P}\mathfrak{B}_d & \cdots & \mathfrak{B}_d^*{\mathfrak{A}_d^*}^{N-1}\mathfrak{P}\mathfrak{B}_d\\
\mathfrak{B}_d^*\mathfrak{P}\mathfrak{A}_d\mathfrak{B}_d & \mathfrak{B}_d^*\mathfrak{P}\mathfrak{B}_d+\mathfrak{F} & \cdots & \mathfrak{B}_d^*{\mathfrak{A}_d^*}^{N-2}\mathfrak{P}\mathfrak{B}_d\\
\vdots & \vdots & \ddots & \vdots\\
\mathfrak{B}_d^*\mathfrak{P}{\mathfrak{A}_d}^{N-1}\mathfrak{B}_d & \mathfrak{B}_d^*\mathfrak{P}{\mathfrak{A}_d}^{N-2}\mathfrak{B}_d & \cdots & \mathfrak{B}_d^*\mathfrak{P}\mathfrak{B}_d+\mathfrak{F}
\end{bmatrix}\\
&P=\begin{bmatrix}\mathfrak{B}_d^*\mathfrak{P}\mathfrak{A}_d & \mathfrak{B}_d^*\mathfrak{P}{\mathfrak{A}_d}^2 & \cdots & \mathfrak{B}_d^*\mathfrak{P}{\mathfrak{A}_d}^N\end{bmatrix}^{\top}\\
&T_u(\cdot)=\begin{bmatrix}\langle{\mathfrak{A}_d}^N(\cdot),\underline{\phi_u}\rangle\end{bmatrix}\\
&S_u=\begin{bmatrix}\langle{\mathfrak{A}_d}^{N-1}\mathfrak{B}_d,\underline{\phi_u}\rangle & \langle{\mathfrak{A}_d}^{N-2}\mathfrak{B}_d,\underline{\phi_u}\rangle & \cdots & \langle\mathfrak{B}_d,\underline{\phi_u}\rangle\end{bmatrix}\\
&U=\begin{bmatrix}u(k+1|k) & u(k+2|k) & \cdots & u(k+N|k)\end{bmatrix}^{\top}
\end{aligned}
\tag{17}
$$

REFERENCES

[1] W. H. Ray, *Advanced process control*. McGraw-Hill: New York, NY, USA, 1981.

[2] E. Davison, "The robust control of a servomechanism problem for linear time-invariant multivariable systems," *IEEE transactions on Automatic Control*, vol. 21, no. 1, pp. 25–34, 1976.

[3] A. A. Moghadam, I. Aksikas, S. Dubljevic, and J. F. Forbes, "Infinite-dimensional lq optimal control of a dimethyl ether (dme) catalytic distillation column," *Journal of Process Control*, vol. 22, no. 9, pp. 1655–1669, 2012.

[4] P. D. Christofides and P. Daoutidis, "Feedback control of hyperbolic pde systems," *AIChE Journal*, vol. 42, no. 11, pp. 3063–3086, 1996.

[5] M. Krstic and A. Smyshlyaev, "Backstepping boundary control for first-order hyperbolic pdes and application to systems with actuator and sensor delays," *Systems & Control Letters*, vol. 57, no. 9, pp. 750–758, 2008.

[6] X. Xu and S. Dubljevic, "The state feedback servo-regulator for countercurrent heat-exchanger system modelled by system of hyperbolic pdes," *European Journal of Control*, vol. 29, pp. 51–61, 2016.

[7] P. D. Christofides, "Robust control of parabolic pde systems," *Chemical Engineering Science*, vol. 53, no. 16, pp. 2949–2965, 1998.

[8] S. Dubljevic, N. H. El-Farra, P. Mhaskar, and P. D. Christofides, "Predictive control of parabolic pdes with state and control constraints," *International Journal of Robust and Nonlinear Control: IFAC-Affiliated Journal*, vol. 16, no. 16, pp. 749–772, 2006.

[9] S. Khatibi, G. O. Cassol, and S. Dubljevic, "Model predictive control of a non-isothermal axial dispersion tubular reactor with recycle," *Computers & Chemical Engineering*, vol. 145, p. 107159, 2021.

[10] D. Dochain, "State observers for tubular reactors with unknown kinetics," *Journal of process control*, vol. 10, no. 2-3, pp. 259–268, 2000.

[11] ——, "State observation and adaptive linearizing control for distributed parameter (bio) chemical reactors," *International Journal of Adaptive Control and Signal Processing*, vol. 15, no. 6, pp. 633–653, 2001.

[12] A. A. Alonso, I. G. Kevrekidis, J. R. Banga, and C. E. Frouzakis, "Optimal sensor location and reduced order observer design for distributed process systems," *Computers & chemical engineering*, vol. 28, no. 1-2, pp. 27–35, 2004.

[13] J. M. Ali, N. H. Hoang, M. A. Hussain, and D. Dochain, "Review and classification of recent observers applied in chemical process systems," *Computers & Chemical Engineering*, vol. 76, pp. 27–41, 2015.

[14] M. Krstić, *Delay compensation for nonlinear, adaptive, and PDE systems*, ser. Systems & control. Birkhäuser, 2009, ch. 1.8: 'DDE or Transport PDE Representation', p. 9.

[15] S. Hiratsuka and A. Ichikawa, "Optimal control of systems with transportation lags," *IEEE Transactions on Automatic Control*, vol. 14, no. 3, pp. 237–247, 1969.

[16] L. Mohammadi, I. Aksikas, S. Dubljevic, and J. F. Forbes, "Lq-boundary control of a diffusion-convection-reaction system," *International Journal of Control*, vol. 85, no. 2, pp. 171–181, 2012.

[17] G. O. Cassol and S. Dubljevic, "Discrete output regulator design for a mono-tubular reactor with recycle," in *2019 American Control Conference (ACC)*, 2019, pp. 1262–1267.

[18] G. Ozorio Cassol, D. Ni, and S. Dubljevic, "Heat exchanger system boundary regulation," *AIChE Journal*, vol. 65, no. 8, p. e16623, 2019.

[19] J. Qi, S. Dubljevic, and W. Kong, "Output feedback compensation to state and measurement delays for a first-order hyperbolic pide with recycle," *Automatica*, vol. 128, p. 109565, 2021.

[20] V. Havu and J. Malinen, "The cayley transform as a time discretization scheme," *Numerical Functional Analysis and Optimization*, vol. 28, no. 7-8, pp. 825–851, 2007.

[21] Q. Xu and S. Dubljevic, "Linear model predictive control for transport-reaction processes," *AIChE Journal*, vol. 63, no. 7, pp. 2644–2659, 2017.

[22] O. Levenspiel, *Chemical reaction engineering*. John wiley & sons, 1998.

[23] P. V. Danckwerts, "Continuous flow systems. distribution of residence times," *Chemical engineering science*, vol. 50, no. 24, pp. 3857–3866, 1993.

[24] B. Moadeli, G. O. Cassol, and S. Dubljevic, "Optimal control of axial dispersion tubular reactors with recycle: Addressing state-delay through transport pdes," *The Canadian Journal of Chemical Engineering*, 2025.

[25] E. Hairer, M. Hochbruck, A. Iserles, and C. Lubich, "Geometric numerical integration," *Oberwolfach Reports*, vol. 3, no. 1, pp. 805–882, 2006.

[26] R. Curtain and H. Zwart, *Introduction to infinite-dimensional systems theory: a state-space approach*. Springer Nature, 2020, vol. 71, ch. 3.2: 'Riesz-spectral operators', pp. 79–108.